Welcome to . . . The Astronomy Zone!

In Which Two D&D Nerds Build a Hydrogen Line Radio Telescope

Contents:

Moonlighting: Overview

Introduction

The exact phrases expressing the excitement that started this project are perhaps not appropriate for general audiences. One of us had successfully used their software defined radio to receive images from orbiting NOAA weather satellites, and was looking for a fun challenge. After wandering through the depths of the radio related internet, the Open Source Radio Telescope website revealed images of a device made of lumber, foam insulation paneling, and fairly standard radio equipment. It was a device designed to investigate the structure and motion of clouds of hydrogen gas across the galaxy, *the galaxy*. Was it really possible? Another link led to the DSPIRA program, using a very similar telescope as part of an NSF program for teachers. It was real! Just one problem: woefully insufficient background in radio astronomy, spectrometry, digital signal processing, or the necessary software. Who cares though, learning by doing is the best way to learn. No sleep was had that night due to excitement and wondering if this could be pulled off in summer. This was too good and too hard not to be shared though, so a late night inquiry was made to a local space-loving physics major and Dungeon Master extraordinaire, and so here we are. Presenting one of the most MacGyvered projects ever: a DIY hydrogen line radio telescope.

Project Goals

- Do fun nerdy stuff with a beloved fellow nerd [✓]
- Learn the basics of radio astronomy and digital signal processing [**?**]

Hydrogen Line Astronomy

Right, so, before getting into all the fun space stuff, let's talk about the hydrogen line. Hydrogen is the most abundant thing in our universe, and mapping the neutral hydrogen using the radiation it gives off can give us a pretty accurate view of what our galaxy looks like.

The radiation comes from the hydrogen's transition between two levels in its ground state, specifically called the 'spin-flip transition'. It's exactly what it sounds like—the hydrogen's proton and electron each have their own spin, and they can either spin parallel or antiparallel to each other. The state with parallel spins is slightly higher in energy, so when the spins flip, it releases that energy as radiation that we can detect (alright, I lied, this is already pretty cool space stuff). We know the frequency the energy is released at (it's around 1420.4 Megahertz), and we also know that this radiation is enough to penetrate through clouds of space dust much better than visible light can, giving us a more complete look at our galaxy.
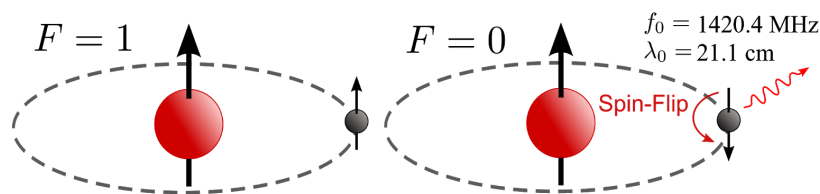

Image: Adapted from Wikipedia

If getting an accurate radio map of our galaxy isn't enough for you, the hydrogen line can also give us information on how the galaxy is moving. When we're viewing an object that's moving towards or away from us, the light that we can observe blueshifts or redshifts—its observable wavelengths get shorter or longer. Since we know at what frequency the radiation was emitted, we know exactly the amount it was blue or redshifted by the time it reaches us. In other words, we can tell if the object we're looking at is moving away from us or closer to us, and, using some less-than-fun (unless you're into that) math, can also figure out how fast it's moving.

Inspiration: DSPIRA and OpenSourceRadioTelescopes

I hope you like acronyms: the Digital Signal Processing in Radio Astronomy (DSPIRA) program is a National Science Foundation (NSF) Research Experience for Teachers (RET) run by the West Virginia University Radio Astronomy Instrumentation Lab (WVURAIL) and the National Radio Astronomy Observatory (NRAO) at the Greenbank Observatory. As is stated in the name, its focus is to provide a research experience for high school teachers that they can then [put to use](#) in the classroom. They provide information on [background concepts](#) in astronomy and DSP, as well as

guided activities in GnuRadio and construction of the horn antenna. If I recall, this was the website that I came across initially that started this ball rolling, so my thanks to them!

Another great reference is Open Source Radio Telescopes (OSRT). While the DSPIRA program website has more information about the astronomical and signal processing background (hence their name), ORST is perhaps the better reference on the hardware and electronics. The reason for this is that they have documented multiple construction variations and the evolution of their construction, electronics, and software setup in the LightWork Memo series. Memos 14 and up are essentially current and so have information that is immediately relevant, but the origins of the project are still interesting.

As far as actually using the telescope, both DSPIRA and OSRT refer to files in the gr-radio_astro repository on Github, which contains the GnuRadio blocks and flowgraphs used in both of their documents. Their procedures on use vary based on which flowchart is being used and so there isn't a unified approach. We have found the procedures for the *spectrometer_w_cal.grc flowgraph* to be the most straightforward.

Software Defined Radio and GnuRadio

A Software Defined Radio (SDR) is a device that is controlled by and interacts with a computer, and is capable of receiving radio data over a huge range of frequencies. So, instead of needing a device designed to receive and demodulate (translate) a specific set of frequencies (87-107 MHz for an FM radio, 2.5 GHz for a wifi receiver, etc.) and signals, you can adjust all of this with a computer. For $22 to $30 you can buy a device and listen in on frequencies from 24 MHz to 1,600 MHz! Airport towers, conspiracy theorists on HAM frequencies, hear shuttle bus drivers and other employees talk trash on people they just dealt with, all yours to discover! With a more money ($200+) you can go from <1 MHz to 6,000 MHz, get better reception quality, and even transmit at low power. If you want to visualize and listen to signals with these devices, either GQRX for Mac/Linux users or SDR# for Windows users. There's a ton of projects you can do with these simple devices on rtl-sdr.com: one favorite is making an antenna to receive satellite imagery!

What if you actually want to DO something with the information you've received? SDR# has some built in tools that I'm guessing are pretty good and easy to use. But, if you really want to get in there and have the ability to create or at least modify things, GnuRadio is probably your best bet. It lets you make radio processing programs by creating flow diagrams between drag and drop blocks that you can edit. These flow diagrams range from the simple (AM radio receiver) to the complex (this project). Like most Open Source things, its biggest strength and weakness are the same: you need to understand what you're doing. There are some great resources to get started learning both the key concepts behind SDRs and GnuRadio *at the same time* in either the excellent video series by the creator of the HackRF SDR, the *Field Expedient SDR* series by Paul and David Clark, and indeed the first several labs in the DSPIRA program (this last fact, combined with the fact DSPIRA and OSRT work in GnuRadio makes it not optional). These first two resources were initially made for the security community and use the HackRF due to its ability to transmit, but the core concepts on receiving and the flowgraphs can be tweaked for any device.

GnuRadio is easiest to install on Linux, can be installed on a Mac using MacPorts with some work, and can't be installed in Windows as far as I know. Virtual Machines are too slow, but a much

better alternative if you won't/can't do one of the above is to run Linux live off of a USB. Basically it leaves your hard drive untouched and uses a USB drive as the hard drive while running off your CPU and RAM like a normal computer; it's pretty cool. [Here](#)'s the process to install Ubuntu, but it can be done for other versions of Linux (*cough*, Kali/Pentoo, *cough*) depending on your hobbies and alignment.

This Document

This is not a how-to guide. DSPIRA and OSRT resources have converged on fairly similar designs, all of which are available in the links above. The intent of this document is threefold:
- Describe *why* the telescope is built the way it is and *how* it works. This isn't done in extreme detail, but rather the underlying ideas are discussed as we understand them, with references to more detailed sources. For information that has been harder to find in freely available resources (e.g. design of optimal horns, the particular polyphase filtering process used) more detail is given, while the opposite is true for concepts that are easy to find information on, regardless of importance to the project (e.g. Fast Fourier Transform).
- Act as a top level document with references to the appropriate resource when it arises in discussion. There is a lot of overlap between resources, and sometimes we have needed a bit here and a bit there to piece together a workable solution. The process of finding precisely where to look in the collection of documents we assembled was time consuming, and not necessarily an option for those who don't have a good chunk of summer break to spend on this.
- Act as a record of what we did, either for us to just see some cool stuff we made, or to show other interested parties.

It is organized as follows:
- Petals to the Metal describes the design of the horn antenna, starting from sizing the waveguide and how that and other constraints feed into the optimal horn design process to determine the final antenna.
- The Crystal Kingdom describes the radio hardware used, moving back from the antenna through the low noise amplifiers, bandpass filters, connectors, and finally the AirSpy R2, ending in estimates of the system noise factor, temperature, and gain.
- The Eleventh Hour describes the GnuRadio flowgraph and how each section contributes to creating an accurate spectrometer.
- The Stolen Century describes what we do with the data, including calibration done on the output values, but focusing on making a galactic rotation curve using Doppler shifts and the tangent point method, intensity maps, etc.
- Story and Song is the conclusion and lessons learned.
- Here There Be Gerblins contains references.

If these section headings make no sense to you, then read [this](#) and go listen to the Balance arc of The Adventure Zone. You'll laugh, you'll cry, you'll play Dungeons and Dragons.

Petals to the Metal: Horn Antenna Design Analysis

Antenna and Waveguide

Neutral hydrogen radiates at 1,420.4 MHz, and similar studies have shown that red and blue shifts of up to 2 MHz in magnitude may be observed. Therefore our goal is to design a horn antenna to receive signals in the range of 1,420.4 ± 2 MHz. The antenna is, at its core, a length of 20 gauge copper wire[1] cut to l=5.25 cm, about a quarter of the wavelength λ =21.1 cm corresponding to 1420.4 MHz. With these values in mind, we look for a waveguide and horn to efficiently direct desired frequencies toward the antenna.

While a custom waveguide could be made, F-style paint thinner cans are frequently used by amateur astronomers, and have a short side length b=10.48 cm (10.4 cm on the interior). The longer side of the aperture is a=16.8 cm.
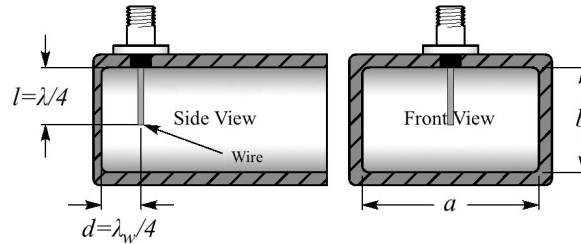
The value of a affects electric fields moving transverse to the antenna, so parallel to the long sides. Crucially, such fields match the antenna polarization and their is independent of the distance from the wall the antenna is mounted on.[2] The cutoff wavelength - the *maximum* wavelength that can propagate in the waveguide in this direction - is λ_c=2a=33.66 cm. This is equivalent to saying the waveguide acts as a high pass filter with cutoff frequency of ν_c=c/λ_c = 891 MHz. Per Condon, in order to minimize dispersion in velocity down the waveguide in the range of interest, a waveguide should be used for frequencies greater than 1.25 ν_c. Additionally, in order to suppress higher order modes they should be used for frequencies less than 1.9 ν_c. The can dimensions thus imply a range of frequencies from 1,114 MHz to 1,693 MHz, containing our observation range of 1,420.4 ± 2 MHz.

While the polarization means that signals moving parallel to the shorter size of the waveguide have less of an effect, it is standard to block such signals for frequencies in our range of interest. $\lambda_{cutoff,b}$ = 2b =20.8 cm, which corresponds to a minimum frequency that can pass in this direction of 1,441 MHz. While this could interfere with some frequencies that our a value allows, it is greater than even the most blue shifted hydrogen line frequencies we are actually observing.

The last calculation that must be made is for the distance d from the back of the waveguide at which to place the antenna. Since the group velocity of propagation down the waveguide differs from that in free-space (due to nonzero path angles required to meet boundary conditions on the edge of the can), we must calculate the *guide wavelength*

$$\lambda_w = \frac{c}{\nu}\left[1 - \left(\frac{\nu_c}{\nu}\right)^2\right]^{-1/2}$$

---

[1] See *LightWork Memo 15*, Figure 2
[2] *Essential Radio Astronomy*, Ch. 3.4 - Waveguides.

This equals 27 cm where ν_c=891 MHz and ν=1420.4 MHz. The antenna should be placed one quarter of this wavelength from the back of the waveguide, at a distance of 6.75 cm.

The above mixture of calculations and materials available lead to the following dimensions:
- Length of longer side of waveguide opening: a=6.625"=16.8cm
- Length of shorter side of waveguide opening: b=4.125"=10.48cm (10.4 cm interior)
- Length of 20 gauge copper wire: l=5.25 cm
- Distance of wire from bottom of waveguide: d=6.75 cm (DSPIRA uses 6.5 cm)

Pyramidal Horn

The horn dimension calculations here follow those of the course notes for lecture 18 of *ECE753 Modern Antennas in Wireless Communications* by Natalia Nikolova. One difference in the design process is that the lecture notes focus on the case of designing an optimal aperture for a desired gain, or perhaps a maximum length. Here the approach is to assume an A value (see diagram below for variable definitions) of just under 30", that is as large as can still fit through a standard door, and design an optimal horn from there and seeing what the resulting gain is.
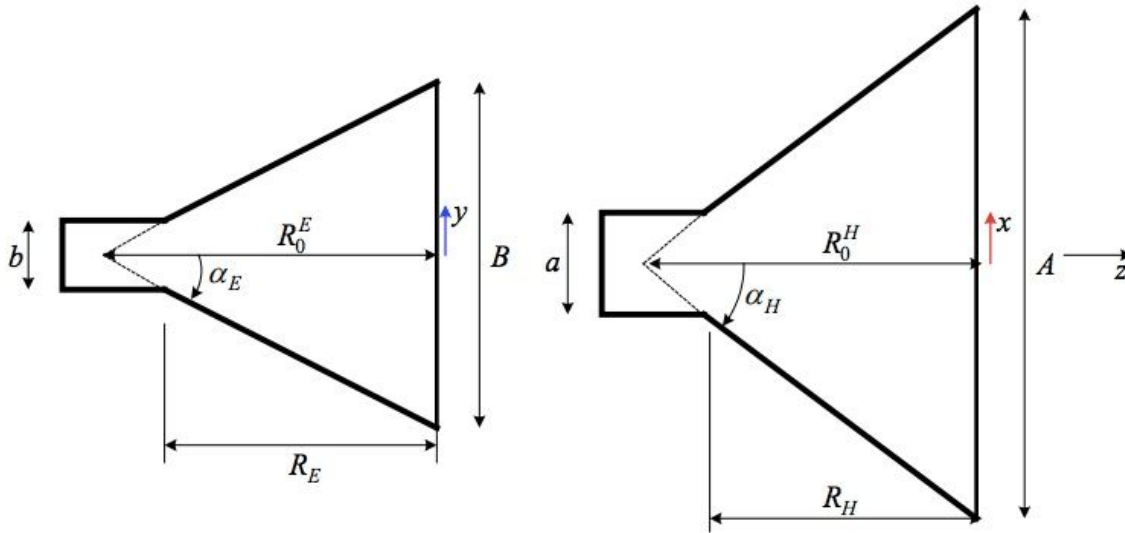
We take A=75.4 cm (just able to fit through a 30" door), and from above a=16.8 cm and b=10.5 cm. For an optimal pyramidal horn, we can calculate B=59.7 cm (The DSPIRA horn is 60.1 cm, which is almost identical and likely due to using imperial units) using

$$B = \frac{1}{2}\left(b + \sqrt{b^2 + \frac{8A(A-a)}{3}} \right)$$

and R_E=R_H=70 cm (The DSPIRA horn is 73 cm per the cutting plan, but realistically 72 cm due to cutting at and angle in order to mount the panels flat due to the thickness of the insulation) using

$$R_H = \frac{A-a}{A}\left(\frac{A^2}{3\lambda} \right) = A\frac{(A-a)}{3\lambda}$$

To summarize the resulting dimensions:
- Length of the longer side of aperture: A=75.4 cm
- Length of the shorter side of aperture: B=59.7 cm (built using 61 cm from DSPIRA)
- Distance from waveguide to aperture opening along panels R=70 cm (built using 72 cm)

Gain and Beam Width

Using the optimum dimensions gives a maximum aperture efficiency of ε_{ap} =.51. The maximum possible gain can be calculated using

$$G = \frac{4\pi}{\lambda^2} \varepsilon_{ap} AB$$.

This gives an ideal gain of 65, or equivalently 18 dB. This is in line with the 18 dB gain found by a group constructing an antenna with nearly identical dimensions[3]. We assume that the slight differences in the DSPIRA design, material imperfections, and construction deficiencies could lead to a loss of up to half of the ideal gain, so the gain in practice somewhat below 18 dB.

The half-power beam width is used to define the beam width of the horn antenna. Numerical simulations for the antenna of nearly identical dimensions in Patel, et al. showed this to occur at 10-12 degrees off-axis depending on the plane, for a beam width of 20 degrees in the H plane (longer side of the aperture, A) and 24 degrees in the E-plane (shorter side of the aperture, B). This in fact aligns with the practical estimates in Condon

$$\theta_{HPBW} \approx 1.2 \frac{\lambda}{D}$$.

where D=A or B depending on the plane in question. This formula gives the beam widths as 19.3 and 24.3 degrees, respectively after converting from radians. The close agreement of simulated values for a similar device and theoretical values for this device suggests the values are close to the actual value. If this is the case, then it should be noted that a 90% power dropoff (10 dB) occurs at 20 degrees off-axis, or a 40 degree beam width.

Another measure of beam width that tried to capture power information in a single 3D cone defined by a single off-axis angle rather than beam widths in two planes is the *solid angle* Ω_A. It is calculated using

$$\Omega_A \equiv \frac{4\pi}{G_0}$$

resulting in a value of Ω_A=11.1 degrees with a peak gain of 63x = 18 dB. This value would increase in proportion to the decrease of the peak gain for reasons other than antenna losses. The solid angle may be used in the analysis of system temperature later on.

In summary:
- Gain: 15-18 dB
- Half power beam width: 20 degrees H-plane, 24 degrees E-plane
- Solid angle: Ω_A=11.1 degrees

---

[3] See the poster *A low-cost 21 cm horn-antenna radio telescope for education and outreach* by Patel, et al.

Pointing Accuracy Requirements and Bias Adjustments

It would be helpful to know how to quantify the effect of pointing inaccuracy on our measurements. The root mean square error, given as a percentage of the total flux density is

$$\frac{\sigma_S}{S} = \frac{z}{(1 + 2z)^{1/2}},$$

where

$$z \equiv 4 \ln 2 \left(\frac{\sigma_2}{\theta_{\mathrm{HPBW}}} \right)^2$$

This gives us a maximum pointing error required for specified accuracy percentage, here being conservative with θ_{HPBW}=20 degrees:

- 5% rms error: 2.8 degrees = .14 θ_{HPBW}
- 10% rms error: 4 degrees = .2 θ_{HPBW}
- 20% rms error: 6.0 degrees = .3 θ_{HPBW}

The above is for the two-dimensional error in pointing angle. This can be converted to maximum errors in *each* angle by dividing by $2^{1/2}$ as follows:

- 5% rms error: 2 degrees = .1 θ_{HPBW}
- 10% rms error: 2.8 degrees = .14 θ_{HPBW}
- 20% rms error: 4.3 degrees = .21 θ_{HPBW}

Along with system noise, an estimate of pointing accuracy can contribute to our error estimates later. Due to construction irregularities, there is a small but visible bias between the horn direction and the frame upon which we can place an angle indicator (mass hanging from string attached to the center of a protractor) and compass to set the elevation and azimuth. We used string to trace straight lines parallel to the frame edges (when viewed face on) along the sides of the horn. We then draw a line on each side running along its center. By measuring the angle between the alignments of the horn and frame, we have determined this bias/offset to be -1º in the horizontal plane (to the right when viewed from above/behind), and -2.7º in the vertical plane (down when viewed from the side). Rather than correct for this bias in calculations, the protractor used to measure elevation with a weighted bob and the mount to place a compass or cell phone to determine the azimuth of the device have been offset by these bias amounts. We estimate this to be accurate to within a degree or two, so when combined with a degree of inaccuracy in reading the protractor or compass angles, a 3º maximum error in each angle seems reasonable, corresponding to 10% rms error in power measurements.

Images
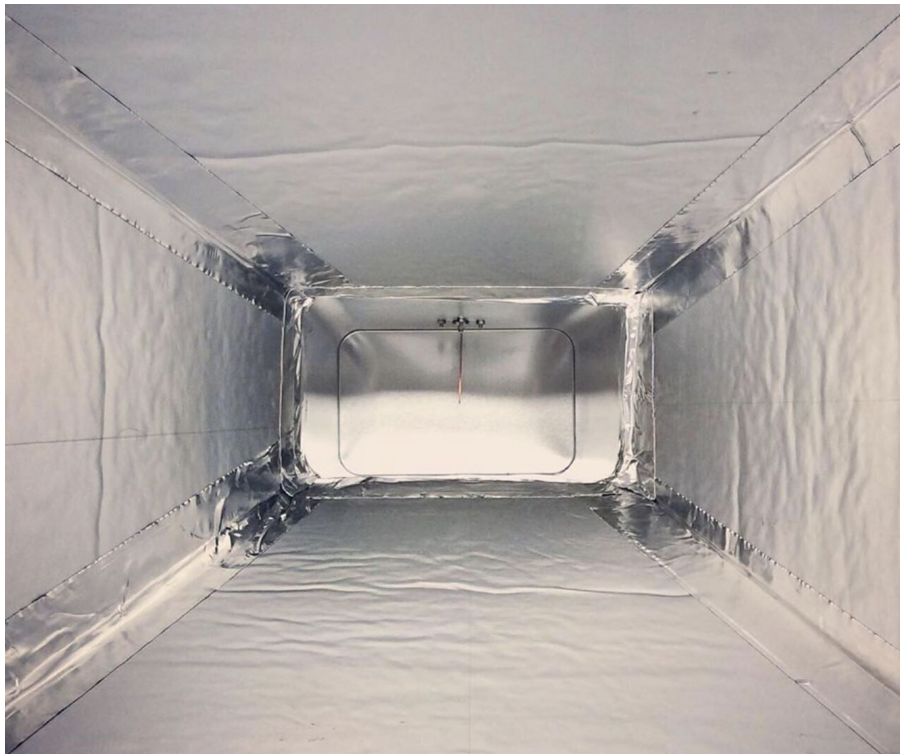
The Crystal Kingdom: SDR, Amplification, and Filtering Setup

When talking about the physical amplification and filtering system hardware, we will focus on its contribution to the gain, noise factor (how much the system decreases the signal-to-noise ratio), and receiver unit temperature.

We assume a .06 dB=.05$(1.4204)^{1/2}$ dB insertion loss per SMA or N-type connection. This value is so low that even across the entire receiving system these add up to approximately 0.5 dB.

The items are listed in order from antenna to SDR:

1. Panel mount N Female connector ([Amazon](#)), soldered to the antenna

2. 90 Degree N Male to Female connector ([Amazon](#))

3. N Male to SMA Male adapter ([Amazon](#))

4. GPIO Labs Hydrogen Line Pre-filtered LNA 1420 MHz ([GPIO Labs](#))

This is an LNA made specifically for Hydrogen Line radio observation. It combines amplification and band-pass filtering in one unit.

Gain values by frequency:

Frequency	Gain
1200 MHz	8 dB
1300 MHz	24 dB
1420 MHz	32 dB
1500 MHz	31.5 dB
1800 MHz	19 dB
2000 MHz	6 dB

Noise Figure: 1 dB

5. 15 cm SMA Male to SMA Male connector ([Amazon](#))

6. 2 x Uptronics 100 MHz to 4 GHz Wideband Preamp ([Uptronics](#))

There are two of these units connected together. The LNA used is a MiniCircuits PSA4-5043 on a spacious and well shielded PCB. The saw filter has been removed to give wideband amplification. A less specialized filter can be used here due to the 20 dB difference in amplification for desired versus undesired powerful frequencies in the preceding GPIO labs unit. It does not appear that there is amplifier saturation with the current setup, though we could certainly experiment with a bandpass filter between rather than after these two units.

Gain values by frequency:

Frequency	Gain
868 MHz	18 dB
1090 MHz	16.7 dB
1415 MHz	15.2 dB

Noise Figure: .75 dB

7. VBF-1445+ Bandpass filter ([Mini-Circuits](#))

This is a simple bandpass filter between an SMA Male and SMA Female connector.

Insertion Loss by Frequency:

Frequency	Loss
1075 MHz	39.44 dB
1180 MHz	21.37 dB
1300 MHz	6.24 dB
1420 MHz	2.23 dB
1470 MHz	2.03 dB
2050 MHz	19.89 dB
2400 MHz	26.38 dB

8. 15 cm SMA Male to SMA Male connector ([Amazon](#))

Summary of Gain and Noise Figure for all pre-SDR elements

We add up the gains and losses for a few frequencies, assuming no amplifier saturation. One of these is of course 1420 MHz, but it is worthwhile to see how much more this frequency is amplified than others to make sure the system does not saturate due to other strong signals.

Total Gain for the LNA/Filter System:

Frequency	Gain
1100 MHz	9 dB
1300 MHz	49 dB
1420 MHz	59.1 dB

Observe that the gain for the target frequency is 50 dB above most other frequencies more than 300 MHz away. Note this final value does not include the gain from the horn antenna of the desired frequency, *nor any attenuation of other frequencies due to the antenna design* (recall it acts as a high pass filter, including blocking the FM band). This leads to a total pre-SDR gain of

$$G_{ant+rx} = 76\text{-}79 \text{ dB, where } G_{ant} = 15\text{-}18 \text{ dB and } G_{rx} = 59.1 \text{ dB}$$

Noise Figure for the LNA/Filter System:

This can be calculated using the Friis formula for noise:

$$F_{\text{total}} = F_1 + \frac{F_2 - 1}{G_1} + \frac{F_3 - 1}{G_1 G_2} + \frac{F_4 - 1}{G_1 G_2 G_3} + \cdots + \frac{F_n - 1}{G_1 G_2 \cdots G_{n-1}}$$

where values are given as ratios, not decibels. For our system:

- F_1 =1 dB = 1.26, G_1 = 32dB = 1585
- $F_2 = F_3$ = 0.75 dB = 1.19, $G_2 = G_3$ = 15.2 dB =33.1

resulting in

$$F_{lna} = 1.2601 = 1\text{dB}$$

It is now evident why people said using cheap line amps were fine for the second and third amplifier. Hopefully the not-inexpensive Uptronics amplifiers will find use as a first stage LNA in other applications. Considering how the Friis formula shows that an LNA significantly reduces the noise of the entire system, reducing the impact of any noisier elements (such as the SDR, see below), they should be used in any application where low noise is desired, even if the SDR's gain is sufficient.

9. AirSpy R2 Software Defined Radio (AirSpy)

Selected Specifications from AirSpy:

- Continuous 24 – 1700 MHz native RX range, down to DC with the SpyVerter option
- 3.5 dB NF between 42 and 1002 MHz* [See note below on tested values for the entire unit]
- Maximum RF input of +10 dBm
- Tracking RF filters
- 35dBm IIP3 RF front end
- 12bit ADC @ 20 MSPS (10.4 ENOB, 70dB SNR, 95dB SFDR)
- 10MSPS IQ output
- 0.5 ppm high precision, low phase noise clock
- 10 MHz panoramic spectrum view with up to 9MHz alias/image free
- No IQ imbalance, DC offset or 1/F noise at the center of the spectrum1 x RF Input
- 4.5v software switched Bias-Tee to power LNAs and up/down-converters* [Unused here]
- Operating temperature: -10°C to 40°C

Configuration:

See the section on signal processing for all of the settings in the osmocom block of GnuRadio used to interact with the device. As just a snapshot, the RF gain is set to 0 (default), while the IF and BB gains are each 12 dB. These very low gain figures show the efficacy of the preceding receiver elements.

Total Receiving System Analysis

Receiving System Noise Figure:

While the company lists the noise figure as 3.5 dB, this is in fact only for the R820T tuner at the front end. Test by various parties have shown an actual noise figure of 4-7 dB.[4] Given the high gain of the set of LNAs and filters above, the noise factor from the Airspy will essentially disappear. So, the total noise factor is still essentially just that of the first LNA from GPIO labs, which is stated to be 1 dB, or a factor of about 1.26. Even if we are a bit suspicious of this value and take the LNA noise figure to be 1.5 dB, this still gives us a ratio of 1.41. *Such a margin could also account for noise introduced from the lack of shielding on our unit.* Thus, we expect final realistic values of

Noise figure: 1-1.5 dB, Noise factor F_{RX}: 1.26-1.41

Recall that this means that all of the electronics, which amplifies the desired signal by more than a million times, only causes an approximately 25% reduction in the signal-to-noise ratio.

Receiving System Noise Temperature

In addition to calculating the noise temperature using observed data from the calibration process, we can also make estimates using the noise figure. Assuming these match, it allows us to validate both the calibration process and the validity of manufacturer data used in the noise factor. To get the receiver noise, we use:

$$T_r = (F_n - 1)\,T_0$$.

This gives us an estimate for the receiving unit temperature of 78 K (using manufacturer numbers) up to 123 K (using 1.5 dB instead of 1 to account for lack or shielding and manufacturer idealism), using T_0= 300 K rather than 290 K due to warm testing conditions.

In order to get this value from our calibration data (discussed in a later section, here we only use the square-law detector output), we use the Y method.[5] It uses the ratio of the hot and cold load detector outputs, along with the actual load temperatures in order to calculate the receiving system temperature.

$$Y \equiv \frac{V_h}{V_c} = \frac{T_h + T_r}{T_c + T_r}, \qquad T_r = \frac{T_h - YT_c}{Y - 1}$$

For example on July 23rd we had a measured output of 132,000 K for cold load temperature of 15 K for the sky,[6] and 450,000 K output for a 300 K hot load.[7] This gives a Y-value of 3.41, and so a receiver temperature of 103 K, about midway in our estimated 78-123 K range. Equivalently:

Measured Noise Figure: 1.27 dB, Measured Noise Factor: F_{RX}=1.34

[4] See http://www.rowetel.com/?p=5867 for more info on the testing procedures used and other results.
[5] Condon, *Essential Radio Astronomy* section 3.6.6
[6] Open Source Radio Telescopes: LightWork Memo 16
[7] It's a bit unclear of what the scaling is here due to the integration, adding in bins, etc., but this cancels in the noise calculation anyways, though it does make it hard to compare the gain.

Images
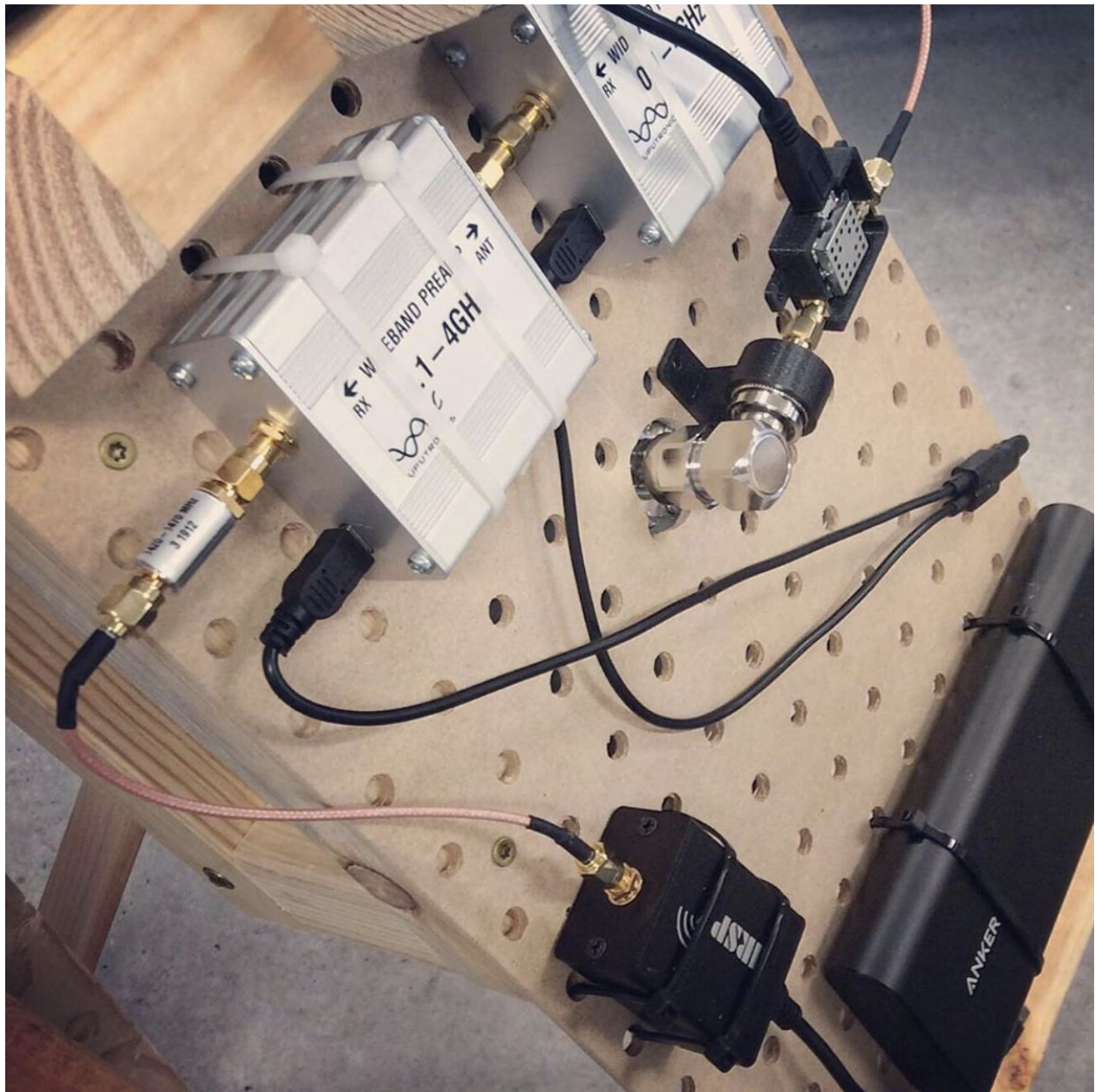
The Eleventh Hour: Finding the Signal in the Noise with GnuRadio

Our goal is to use measurements of 21 cm radio waves to glean information about their sources. Depending on our goals for a set of observations, we are focused on the size, density, and/or velocity of the emitting structures. While the particular manner of extracting this information will be covered in the next section, all of them depend on the measured *power spectral density,* which is the power per unit frequency, given as a function of the frequency.[8] Therefore our goal in GnuRadio is to make a *spectrometer* that covers values near 1420.4 MHz.

Over our observation timescales, we consider the power transmitted by the observation region to be constant, mixed with white noise from a variety of sources. Therefore the received signal can be considered wide sense stationary. For such systems the power spectral density is

$$P_\nu(\nu) = E[|X(\nu)|^2],$$

where $X(\nu)$ is the frequency domain representation of the measured signal (i.e. the *Fourier Transform* of the time domain signal) and E[] stands for the expected value.[9] This definition actually defined the core process that GnuRadio must perform:

1. Calculate the Fourier Transform $X(\nu)$ of the input signal to get its frequency representation.
2. Calculate the square of the magnitude $|X(\nu)|^2$ of the Fourier Transform.
3. Calculate the mean over a sufficiently long time interval in order to approximate $E[|X(\nu)|^2]$.

There are additional steps that need to be performed such as sampling the data, preprocessing to get cleaner results, calibrating the data, etc. These in fact make up most of the flowgraph in GnuRadio, but these all act in support of the core spectrometer.
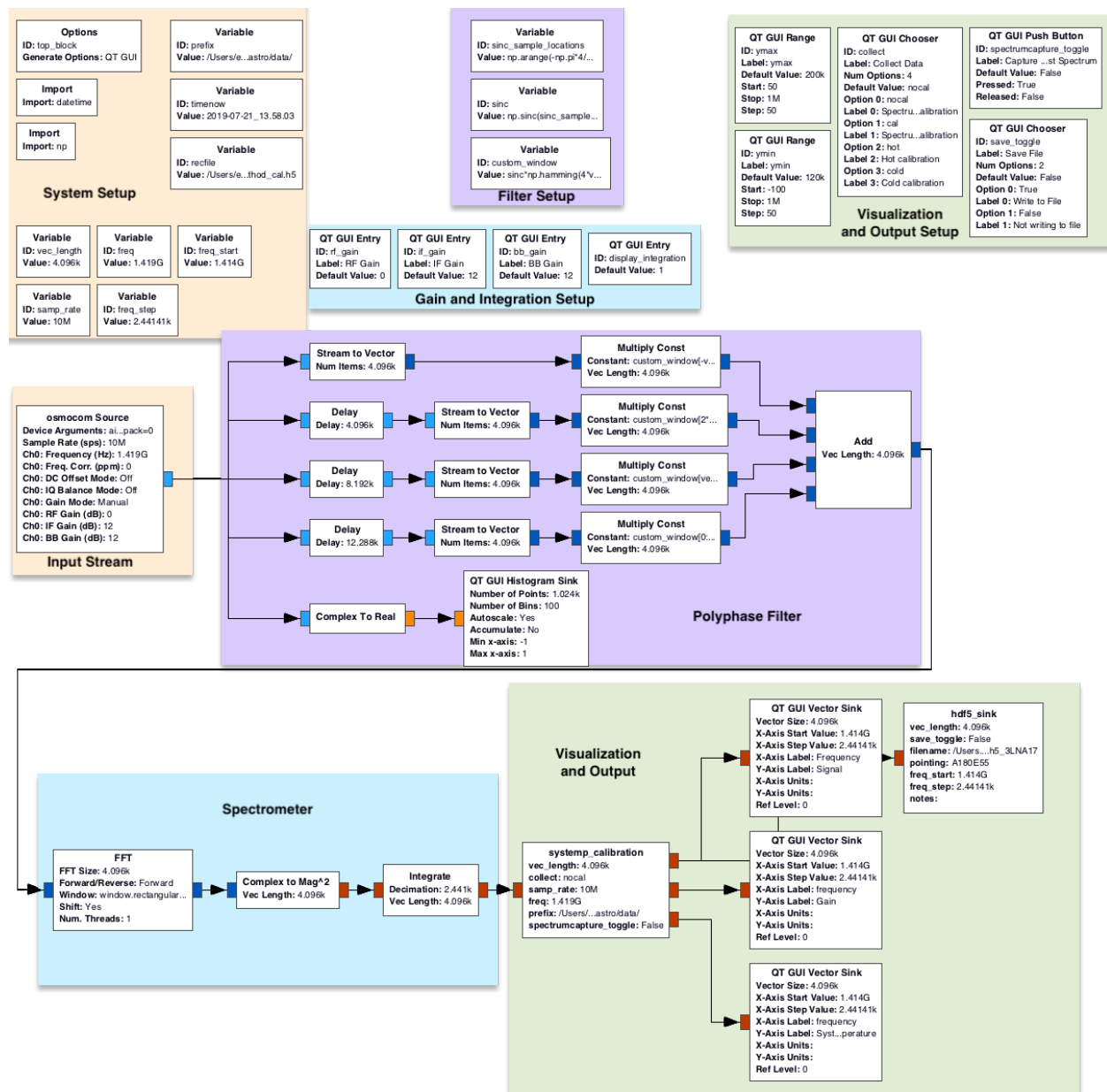
Flow Graph Overview

Before going into the details of each section of the process, the complete GnuRadio flowgraph is shown below. For clarity, the flowgraph has been organized into color coded and labeled blocks, with a section of the flowgraph and the variables that define/affect it having matching colors. It is a modified version of the spectrometer_w_cal.grc flowgraph that is part of the gr-radio_astro package provided by WVURAIL, with the changes described below.

The rest of this section is organized by color coded section: input stream, polyphase filter, and spectrometer. The Visualization and Output section will be discussed in the section on Data Analysis since it involves the calibration process and depends on the particular application.

---

[8] There is some ambiguity in the term between its use in physics where it is indeed related to actual power and thus has units W/Hz, and in signal processing where it is used to refer to a term based on the square of whatever the input signal is measured in. For example, for signals classically measured in volts, the term power spectral density is often in units V^2/Hz. It is understood that these two uses of the term are proportional to each other, and for traditional radios one may be recovered from the other. For SDRs the signal is just scaled values, and "power" is relative to a signal that after scaling would have a constant magnitude of 1, whatever 1 means for that unit and setup. It is quite annoying that this fact is not made more explicit.

[9] See for example, A.7 in Condon, or Section 5.4 of DSPIRA Lab 5.

System Setup

Options
ID: top_block
Generate Options: QT GUI

Import
Import: datetime

Import
Import: np

Variable
ID: prefix
Value: /Users/e...astro/data/

Variable
ID: timenow
Value: 2019-07-21_13.58.03

Variable
ID: recfile
Value: /Users/e...thod_cal.h5

Variable
ID: vec_length
Value: 4.096k

Variable
ID: freq
Value: 1.419G

Variable
ID: freq_start
Value: 1.414G

Variable
ID: samp_rate
Value: 10M

Variable
ID: freq_step
Value: 2.44141k

Filter Setup

Variable
ID: sinc_sample_locations
Value: np.arange(-np.pi*4/...

Variable
ID: sinc
Value: np.sinc(sinc_sample...

Variable
ID: custom_window
Value: sinc*np.hamming(4*v...

Gain and Integration Setup

QT GUI Entry
ID: rf_gain
Label: RF Gain
Default Value: 0

QT GUI Entry
ID: if_gain
Label: IF Gain
Default Value: 12

QT GUI Entry
ID: bb_gain
Label: BB Gain
Default Value: 12

QT GUI Entry
ID: display_integration
Default Value: 1

Visualization and Output Setup

QT GUI Range
ID: ymax
Label: ymax
Default Value: 200k
Start: 50
Stop: 1M
Step: 50

QT GUI Range
ID: ymin
Label: ymin
Default Value: 120k
Start: -100
Stop: 1M
Step: 50

QT GUI Chooser
ID: collect
Label: Collect Data
Num Options: 4
Default Value: nocal
Option 0: nocal
Label 0: Spectru...alibration
Option 1: cal
Label 1: Spectru...alibration
Option 2: hot
Label 2: Hot calibration
Option 3: cold
Label 3: Cold calibration

QT GUI Push Button
ID: spectrumcapture_toggle
Label: Capture ...st Spectrum
Default Value: False
Pressed: True
Released: False

QT GUI Chooser
ID: save_toggle
Label: Save File
Num Options: 2
Default Value: False
Option 0: True
Label 0: Write to File
Option 1: False
Label 1: Not writing to file

Input Stream

osmocom Source
Device Arguments: ai...pack=0
Sample Rate (sps): 10M
Ch0: Frequency (Hz): 1.419G
Ch0: Freq. Corr. (ppm): 0
Ch0: DC Offset Mode: Off
Ch0: IQ Balance Mode: Off
Ch0: Gain Mode: Manual
Ch0: RF Gain (dB): 0
Ch0: IF Gain (dB): 12
Ch0: BB Gain (dB): 12

Polyphase Filter

Stream to Vector
Num Items: 4.096k

Multiply Const
Constant: custom_window[-v...
Vec Length: 4.096k

Delay
Delay: 4.096k

Stream to Vector
Num Items: 4.096k

Multiply Const
Constant: custom_window[2*...
Vec Length: 4.096k

Delay
Delay: 8.192k

Stream to Vector
Num Items: 4.096k

Multiply Const
Constant: custom_window[ve...
Vec Length: 4.096k

Delay
Delay: 12.288k

Stream to Vector
Num Items: 4.096k

Multiply Const
Constant: custom_window[0:...
Vec Length: 4.096k

Add
Vec Length: 4.096k

Complex To Real

QT GUI Histogram Sink
Number of Points: 1.024k
Number of Bins: 100
Autoscale: Yes
Accumulate: No
Min x-axis: -1
Max x-axis: 1

Spectrometer

FFT
FFT Size: 4.096k
Forward/Reverse: Forward
Window: window.rectangular...
Shift: Yes
Num. Threads: 1

Complex to Mag^2
Vec Length: 4.096k

Integrate
Decimation: 2.441k
Vec Length: 4.096k

Visualization and Output

systemp_calibration
vec_length: 4.096k
collect: nocal
samp_rate: 10M
freq: 1.419G
prefix: /Users/...astro/data/
spectrumcapture_toggle: False

QT GUI Vector Sink
Vector Size: 4.096k
X-Axis Start Value: 1.414G
X-Axis Step Value: 2.44141k
X-Axis Label: Frequency
Y-Axis Label: Signal
X-Axis Units:
Y-Axis Units:
Ref Level: 0

hdf5_sink
vec_length: 4.096k
save_toggle: False
filename: /Users...h5_3LNA17
pointing: A180E55
freq_start: 1.414G
freq_step: 2.44141k
notes:

QT GUI Vector Sink
Vector Size: 4.096k
X-Axis Start Value: 1.414G
X-Axis Step Value: 2.44141k
X-Axis Label: frequency
Y-Axis Label: Gain
X-Axis Units:
Y-Axis Units:
Ref Level: 0

QT GUI Vector Sink
Vector Size: 4.096k
X-Axis Start Value: 1.414G
X-Axis Step Value: 2.44141k
X-Axis Label: frequency
Y-Axis Label: Syst...perature
X-Axis Units:
Y-Axis Units:
Ref Level: 0

Input Stream

The AirSpy R2 has a sample rate of 10 MBps that is not really negotiable. This means the bandwidth is 10 MHz, so that the maximum deviation from the center frequency is half the sampling rate, in fulfillment of the Nyquist-Shannon Sampling Theorem. The external amplifiers are all powered over USB, to bias=0 is added to the device description to turn off the bias tee. While the SDR gains are technically part of the Input Stream setup, they were adjusted based on observation of the power spectral density, and are discussed in the Spectrometer section even though they enter the flowgraph here.

Polyphase Filter

We assume the reader has familiarized themselves with the basics of Fourier Transforms and the FFT, and has a notion of that a spectrometer uses these to make a sort of histogram that divides the frequency domain into a set of small bins and shows how much power was received in each bin. There are a few useful facts that we'll use here:. First is that the transform of the product of functions is equal to the convolution of the transforms: $\mathcal{F}(fg)=F*G$. Second is that rectangular (boxcar) functions which are constant on an interval and zero otherwise has as its transform a scaled sinc function, and vice-versa.

(a)

(b)
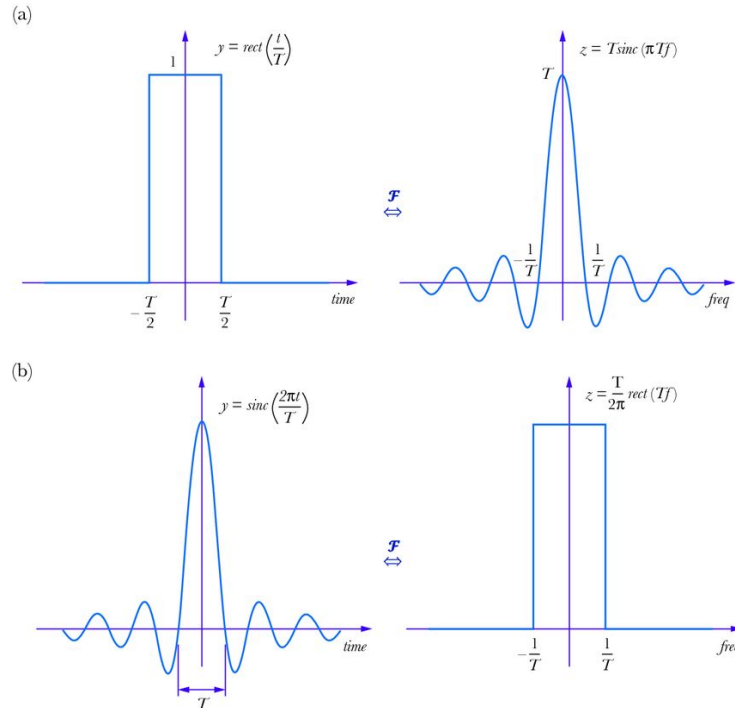
Lastly, when a Fast Fourier Transform is performed, it is not done on the entirety of the signal for all time, rather on some number of the most recent points. In other words, it is applied to the original signal multiplied by a boxcar function.

Consider as well that the continuum of possible spectra is divided into a finite number of values, each representing a small "bin" of frequencies. For each bin (which are all the same size), what we would like is all frequencies within that bin weighted evenly and no frequencies outside of that bin included. What we get instead by multiplying the input signal by a boxcar function is that $X(\nu)$ is convolved with a sinc function centered on each bin, (which shows up in P_ν as $sinc^2$). This has two effects, one is that whenever the sinc function is nonzero at the center of neighboring bins, frequencies within one bin can show up in another bin. This is called *spectral leakage*. Also, the curved shape of the sinc function means not all frequencies within a bin are represented equally; this is called *scalloping loss*.

Returning to the ideal case where for each bin we would like is all frequencies within that bin weighted evenly and no frequencies outside of that bin included. So, what we want is $X(\nu)$ convolved/multiplied (both boxcar and sinc functions are even, so we can be loose with this) with a

boxcar function. But since a boxcar function is the Fourier Transform of a sinc function, this implies we should multiply our original function by a sinc function (or at least something close to it since sinc functions go off infinitely in both directions).
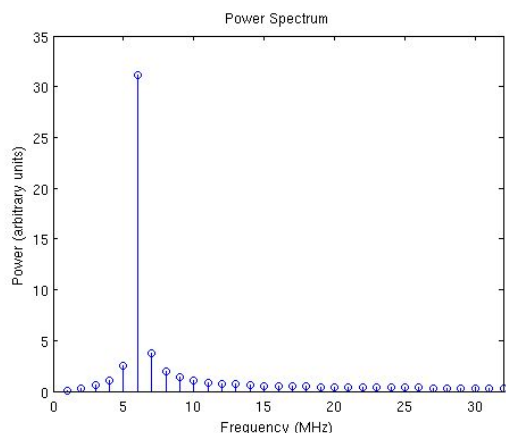
A 5.1 MHz tone convolved with a sinc function leads to spectral leakage[10]

Let n equal the number of bins in the FFT. Bin width is bandwidth/n = sample_rate/n, so the half-width is sample_rate/($2n$). Each bin is then the Fourier transform of a sinc function whose distance between the first zeros is $2n$/sample_rate, but which continues off in both directions with decreasing magnitude. We can only sample for a finite time, so instead of the small window defined by the first zeros of the sinc function, we instead truncate at twice this distance, so a width of $4n$/sample_rate, which is equivalent to $4n$ samples. Since we cannot look into the future, the sinc function is centered halfway in this larger sample set, as shown below[11] for the case n=256.
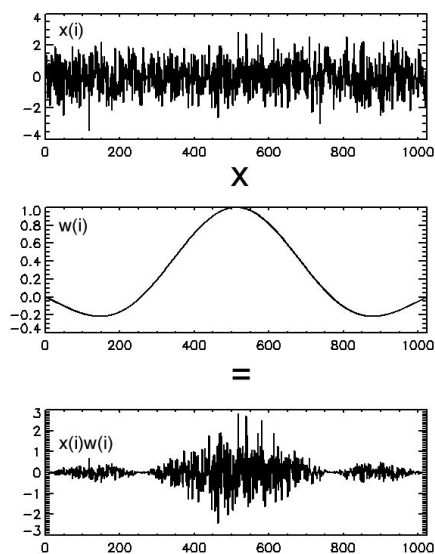
We are left with the issue that the FFT operates on as many samples as there are bins. To fix this, the resulting signal is cut into four pieces, each with a number of samples equal to the number of bins in the FFT, and then these are added together.

---

[10] This image is from DSPIRA Lab 5
[11] This image and the next image are from Physics 728 Lecture Notes, Lecture 8 by Dale E. Gary.
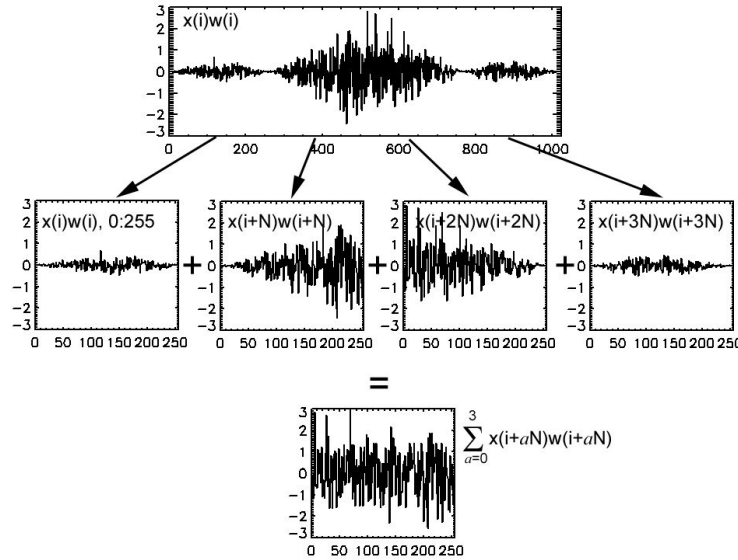
This last step is a mixture of shifting (does not change power), multiplying by boxcar windows, and then adding back together, and is a sort of weighted moving average. While we have established that multiplying a signal by a boxcar isn't great, multiplying the signal by both a sinc and a boxcar results in the final FFT being convolved with the convolution of a sinc function and a boxcar function, rather than just a sinc function. This serves to "square off" the edges, reducing both spectral leakage and scalloping loss, as shown below[12] (note the shift to a logarithmic scaled y-axis) where PFB represents the above approach and FFT the standard Fast Fourier Transform. Judicious shaping of the sinc function can align the edges with the edges of the bins.
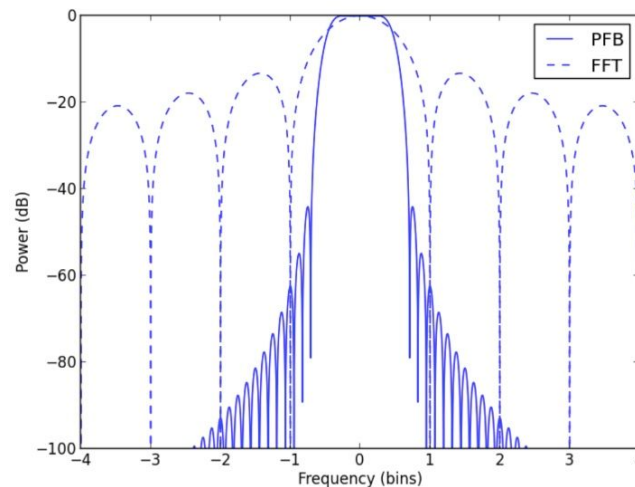
In GnuRadio, the variables associated with the Polyphase Filtering define the sinc function shape. The delay blocks serve to split the stream into four consecutive chunks, each with a number of samples equal to the number of bins in the FFT. The multiplication by the correct part of the sinc function is made, and the results added together like in the diagram at the top of the page.

---

[12] This image is from DSPIRA Lab 5

Spectrometer

Calculate the Fast Fourier Transform $X(\nu)$:

The preceding section was an overly long detour included because the precise method used isn't included in many (any?) books that I found, just in a couple PDFs. The FFT, however, is everywhere, so look it up. It's fast *and* fun, just not to write about. GnuRadio has an *FFT* block, so that gets used. The Polyphase Filtering takes care of improving the results and so rectangular windowing is selected in the options, as that is compatible with the approach above. *Practical Digital Signal Processing* is relatively light reading, but there are *many* free resources.

One adjustment made from the original spectrometer_w_cal.grc was reducing the size of the FFT from 4,096 to 2,048 or 1,024 bins. 1,024 bins increases the bin size to approximately .01 MHz (10 MHz/1024), which we'll see later on corresponds an uncertainty in relative velocity of about ±1 km/s per bin, which is less than the expected error due to other sources. This is more than made up for due to the increased spatial averaging due to more samples being included in the bin. It also increases the number of data sets processed by the integrate block per second, described below. This sixteen fold increase in the number of samples average should lead to a four-fold decrease in the standard deviation of the noise. This is seen below in two <u>uncalibrated</u> measurements in a noisy environment with the only change being the change in FFT size mentioned above (1 s collect).
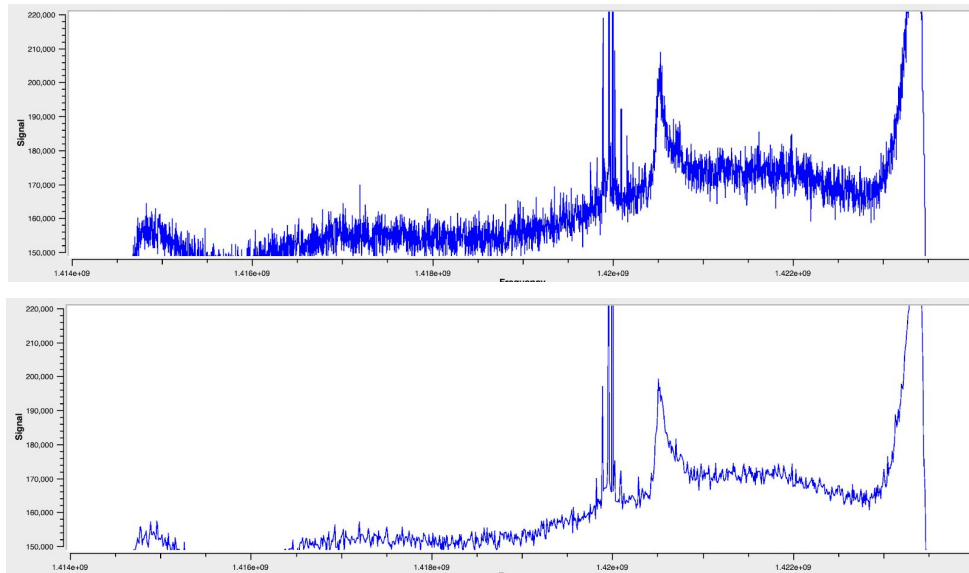

Calculate the Magnitude Squared $|X(\nu)|^2$:

GnuRadio has a *Complex to Magnitude^2* block, so I used that. You could alternatively multiple the FFT output by its complex conjugate and converting to real, which does the same thing. That makes the underlying math more clear, but in an already large flowgraph I thought the explicitness was helpful.

Average to Approximate $E[|X(\nu)|^2]$:

This is a key part of the process since the noise is generally larger than the signal. However, since it is nearly zero mean white noise once we have calibrated, when you add/average the data over time the noise cancels itself out, allowing the signal to emerge.

The *Integrate* block sums the number of samples contained within the number of seconds given by the display_integration variable (and in effect causing a decimation in the number of samples passed through by the same factor). It does not, however, divide by that number to get the mean. One can either modify the flowgraph to divide by the number of samples in the integration time, or rely on the fact that this is eliminated in the calibrated data by being factored into the gain. The former has a benefit in that the user does not need to adjust the graph scaling for uncalibrated data when changing the integration time. Note that the original spectrum_w_cal.grc file had another integration variable, but it was in fact unused -- a fact discovered after adjusting it to no result. It has been removed from the updated file. Increasing this value does create improvements in noise reduction, but causes significant lag. 1,024 bin FFTs with integration time 1 s and 4 s are shown below.
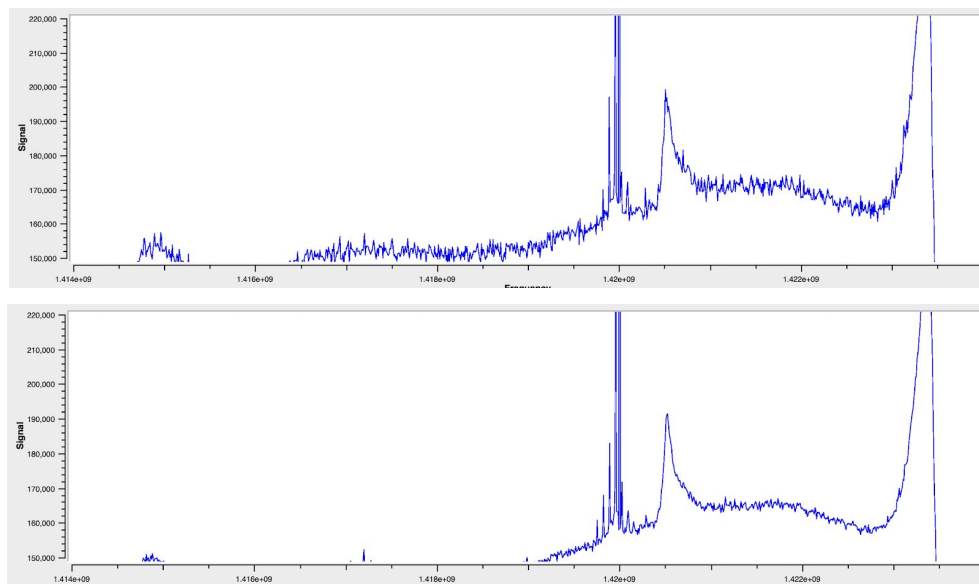
Gains:

While the SDR gains are technically part of the Input Stream setup, they were adjusted based on observation of the power spectral density here. I set the RF gain (the broadband hardware amplification in the device) to 0 as a default when first evaluating gain values in order to protect the system from too strong of a signal[13]. The intermediate frequency and baseband gain did not need to be raised very high since the signal was quite prominent due to external amplification, so they were adjusted until the uncalibrated spectrum values were similar to those I have seen in other successful projects.

Essential Radio Astronomy Ch.3.6 discusses the ideas behind radiometers and spectrometers in radio astronomy applications, with Ch.7 dedicated to systems studied by such methods.

---

[13] Per the suggestion of Michael Ossman, creator of the HackRF SDR. See the educational series on the Great Scott Gadgets website: https://greatscottgadgets.com/sdr/.

The Stolen Century: Data Collection and Analysis

Preliminary Rant: Units for Calibrated Data and System Noise

The calibration process (described in detail in the final subsection of [The Crystal Kingdom: SDR, Amplification, and Filtering Setup](#)) uses the raw antenna measurements of relatively empty sky and the ground, along with their actual temperatures, to determine the system noise and a gain value. The program then uses these to get a calibrated measurement of the inputs into the antenna. For example, compare the uncalibrated frequency domain plots in the previous section to the calibrated data below.
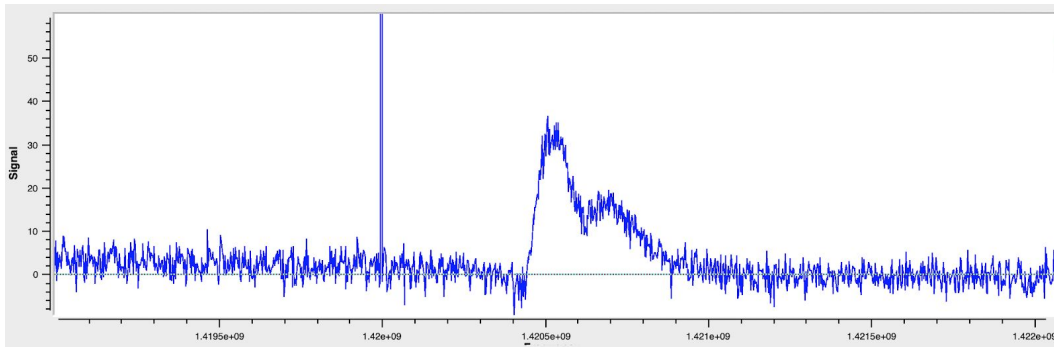
Calibrated Data w/ a 4,096 point FFT and 4s integration time, pointing at Mirfak. Galactic lat,long = (-5.86, 146.57) degrees

An obvious question would be *what are the units?* Well, that's a bit complicated. Since the result of the FFT is the power spectral density (power per unit frequency), we'd expect units of W/Hz. Instead, astronomers generally use temperature in Kelvin. Let's repeat that: temperature in Kelvin. Specifically, _the temperature of a matched resistor (one whose resistance matches the impedance of the antenna, so 50 Ω) that would generate an equivalent amount of power as the antenna is receiving_.[14] The relationship between power spectral density and this temperature is given by

$$P_\nu(\nu)=kT(\nu)$$

where $k=1.38\times10^{-23}$ m^2 kg s^{-2} K^{-1} is Boltzmann's constant.

It's tempting to just give a Gallic Shrug when asked why would anyone use this as the choice of units, but here's the usual justifications.

1. Since Boltzmann's constant is very small, using temperature gives much smaller / finer grained unit. Therefore instead of very small values in units of power associated with astronomical observations, one gets easier to read units of temperature.
2. This is exactly the same unit astronomers use to measure the system noise instead of the more intuitive noise factor. So, we can directly compare signal strength vs noise of the receiver, atmosphere, etc. Recall our receiver noise estimate is 100 K.
3. There are relationships between the antenna temperature and the brightness temperature of the emitting object based on what percentage of the solid angle the object takes up.

---

[14] Condon, *Essential Radio Astronomy,* section 3.6

Some sassy comments: The problem with small numbers that item 1 tries to solve is really an astronomy issue. Higher power applications are happy to use power. The signal to noise analysis that item 2 allows can of course also be done with noise factor/figure and power, so that may not be as big of a deal as people make it. For item 3, brightness temperature only directly applies to blackbody radiation (e.g. stars, cosmic background radiation), which is not what we are dealing with here with the H_I transition. Instead, astronomers use an *equivalent* brightness temperature for non-thermal radiation. To this observer, it looks like astronomers were trained first on blackbody radiation in the visible spectrum and just didn't feel like changing units when moving to radio, and now it's just entrenched. Regardless, the units are temperature of an imaginary resistor in Kelvin.

Less Annoying Preliminaries: Galactic Coordinates

Since most of our observations are based on galactic coordinates, the image below will be helpful both to show the coordinate system and show the reader a map of the structure of the galaxy as currently understood. It is shown looking down from the galactic North pole.
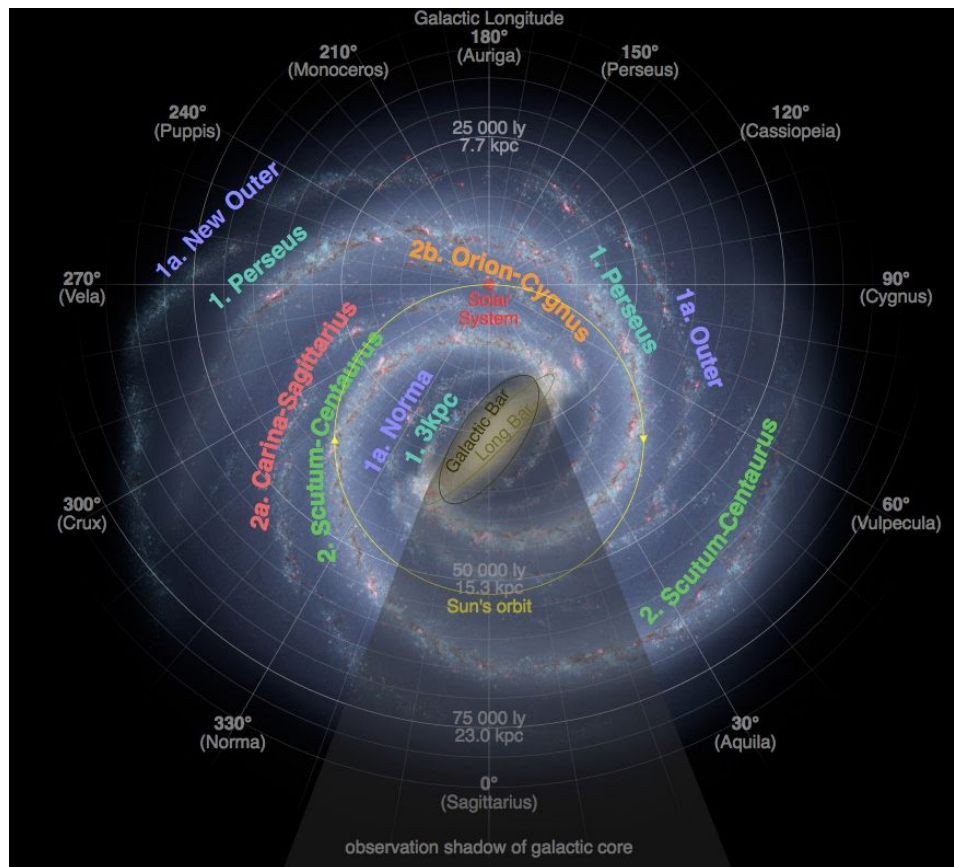

The coordinate system has the Sun at its origin. The galactic equator is perpendicular to the axis of rotation of the galaxy as a whole. Galactic latitude is the angle above or below the galactic equator (the direction of galactic north being the half of the rotational axis closest to our north, even though they are offset by a sizeable 61° difference) The line from the Sun to the center of the

galaxy defines galactic longitude 0°, with numbers increasing as one moves in a counterclockwise direction, as seen from the galactic North.

There are online tools or scripts in Python that perform transformations between azimuth/elevation, right ascension/declination, and galactic coordinates, provided the time and observer position are known as well.

A Qualitative Description of a Single Spectrum

Let's return for a moment to the spectrum pointing in the direction of Mirfak in July 2019, with galactic (lat,long) = (-5.86, 146.57).
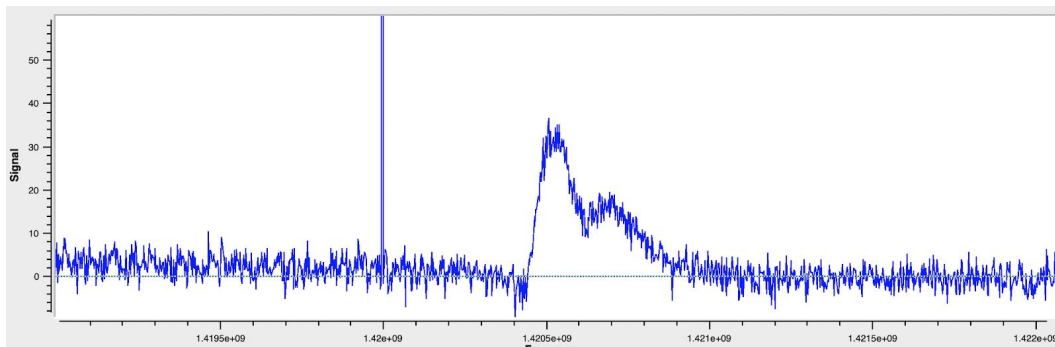
A galactic longitude of 146.57° means we are pointing away and a bit clockwise from the galactic core (see the map of the galaxy above).

The first thing to note is that relative to the emission frequency of 1420.4 MHz, the received signal has been blue shifted. Given that angular velocity decreases with distance and the direction we are pointing is slightly clockwise, we will be 'catching up'/moving toward these more distant parts of the galaxy if the galaxy is rotating clockwise (as seen from the galactic North), or moving away from these regions if the galaxy is moving counterclockwise. This may sound odd given that we are visualizing things as rotating in a circular fashion, but think about how the Earth moves closer to and then further away from Mars repeatedly due to the higher angular velocity of the Earth, even though both planets still maintain their orbits. The precise relationships will be discussed in the next section, but the observed blueshift means we are moving relatively toward that part of the galaxy, thus the galaxy is rotating clockwise. Looking at the map of the galaxy and seeing the direction the spiral arms are trailing, we can see this matches current understanding.

The next thing to note is that there is a peak, then a valley, and then another peak further out with greater blue shift. Our relative velocity is greater for objects that are further away, so this suggests close proximity to a large amount of hydrogen gas, then a gap, and then more gas. If this trend were to continue for other longitudes (it does), it would suggest that instead of a smooth distribution of gas, our galaxy has a banded or arm structure. As can be seen on the map of the galaxy, this is indeed the case. We believe the first and highest peak is from our own Orion Spur, while the second is the Perseus Arm. Note the wider spread of frequencies and hence relative velocities for the Perseus arm. This suggests that the arm is wider than however much width of the Orion Spur remains in this direction. Again, looking at the map we see this to be the case. A bunch of lumber and insulation from Home Depot can see the spiral arms of the galaxy!

One question raised is why the first peak doesn't start at 1420.4 MHz, but rather 1420.5 MHz? Shouldn't gas at the nearly the same distance from the center of the galaxy be moving at nearly the same speed and so show no blue shift until we move further out in the Orion Spur? One possibility is that there isn't much neutral hydrogen near us and that it is all ionized, in stars, etc. Another takes into account that while galactic coordinates are centered on the Sun, but we're on a moving planet. At the time of the measurement, the Earth was approximately at galactic longitude 20° (in July the galactic core is nicely visible at night in the Northern Hemisphere, meaning we are roughly between the Sun and the galactic core), with the projection of its velocity on the galactic plane being up and to the right (roughly 110°) as seen on the map, hence somewhat toward objects in our line of sight. This means the motion of the Earth should blue shift everything in the line of sight a little bit, even gas that would have no blue shift if seen from the Sun. If you do the math using the formula in the next section, the blue shift at the left edge of the first peak corresponds to a relative velocity (20 km/s) roughly equal to the component of the Earth's velocity in the direction of our line of sight (a bit less than 24 km/s since the motions aren't coplanar).

So there you have it, in one graph you can see that the galaxy is rotating clockwise, that it has a banded or arm structure, that the next arm further out is pretty beefy, and that you can see the effects of the Earth's motion on the results. That is a lot of information from an almost totally qualitative analysis of a single spectrum. When you actually apply the math and start linking observations together, that's when things get really interesting.

Our Primary Science Objective: The Galactic Rotation Curve

The following sections break down the lengthy process behind our primary science objective, which is to analyze the speed of the rotation of the galaxy as a function of distance. Aside from the nature of the rotation being a subject of interest in its own right, it is particularly interesting when results are compared to predictions based on the distribution of visible matter within the galaxy. As we'll see, there's definitely something missing from that picture of the galaxy, and indeed, the universe.

To summarize the process, we are assuming that for most of the galaxy we can closely describe the rotation using uniform circular motion. Using the amount of blue or red shifting, we can calculate the relative velocity of different regions of neutral hydrogen gas. Furthermore, for certain ranges of galactic longitude, we can also calculate the distances at which some of these speeds occur. With distance and relative velocity now in hand, some trigonometry will allow us to get the speed of rotation as a function of distance from the galactic core.
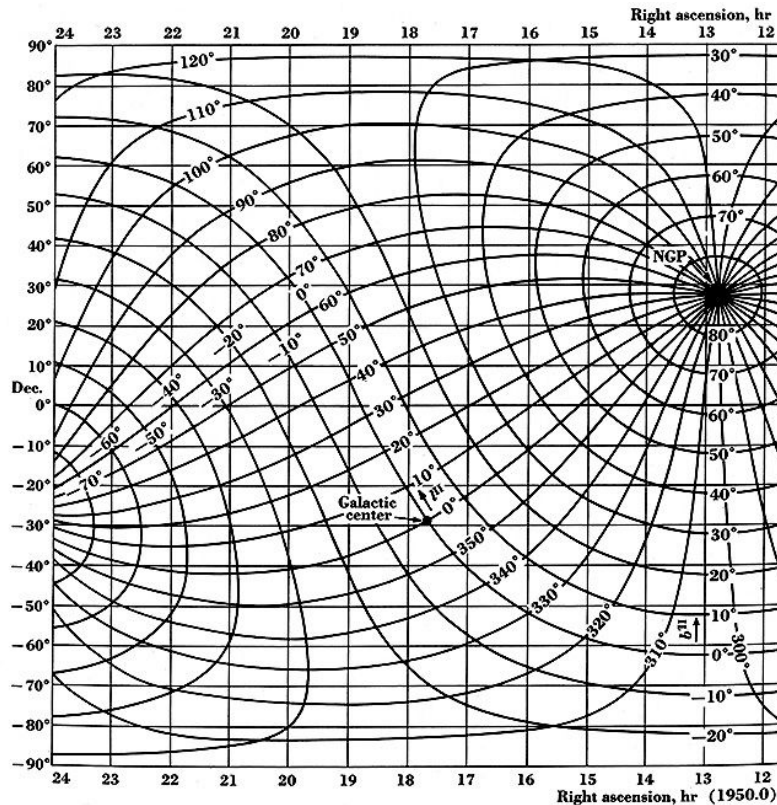
The Galactic Rotation Curve: Observation Plan

While the trigonometry used in the tangent point method below is valid for any angle $-90 < \theta < 90$, there are a few practical limitations that reduce our observation range to galactic longitudes in the range $25^{\circ} < \theta_i < 75^{\circ}$. Closer to the galactic core the validity of using uniform circular motion to approximate the motion of the H I gas clouds becomes invalid. For angles closer to 90°, the observed blue/red shift is dominated by local, smaller scale motion as the difference in distances from the galactic core approaches 0. Lastly, the exclusion of negative galactic longitudes is due to

being in the northern hemisphere. As our measurements are explicitly for motion in the galactic plane, galactic latitude is 0° in all cases. We will observe values in this range that are 10° apart, corresponding to our half-power bandwidth.

The table below provides these locations in both galactic coordinates and the more common right ascension and declination of the equatorial celestial coordinates.

Galactic Lat.	Galactic Long.	RA (deg)	Dec (deg)	RA (h/m/s)	Dec (d/m/s)	Nearby Star or Object
0	25	279.224	-7.055	18h36m54s	-07d03m16s	M26
0	35	283.803	1.840	18h55m13s	+01d50m26s	Alya
0	45	288.428	10.724	19h13m43s	+10d43m25s	Okab
0	55	293.333	19.535	19h33m20s	+19d32m04s	M71
0	65	298.803	28.198	19h55m13s	+28d11m52s	Albireo
0	75	305.229	36.606	20h20m55s	+36d36m20s	Al Fawaris

These conversions can be found using online calculators, Python code, or the following conversion chart:

The Galactic Rotation Curve: Doppler Shift

Doppler Shift is the change between the wavelength emitted and the wavelength observed due to relative between the source and the receiver. Humans are familiar with the changing pitch of a moving vehicle. For light, this change is given by

$$\frac{\lambda_o - \lambda_e}{\lambda_e} = \frac{\Delta\lambda}{\lambda} = \frac{v}{c}$$

where $c=3.0\text{x}10^8$ is the speed of light, v the relative velocity, λ_e the emitted wavelength, and λ_o the observed wavelength. Using the relationship $\lambda = cf$, we can reframe this in terms of frequency as

$$\frac{f_e - f_o}{f_o}c = v$$

The reason this whole process works is that we know the precise value of the emitted frequency for any neutral hydrogen gas undergoing the superfine transition: f_e=1420.40575 MHz. Since we know this value and the speed of light, for any received frequency we can calculate the exact relative velocity of the emitting hydrogen gas cloud relative to us. The trick is then to figure out which frequencies on the spectrum will allow us to find not only the relative velocity, but also its distance from the galactic core.

The Galactic Rotation Curve: Tangent Points

As can be seen in the multiple spectra shown previously, there is a wide variety of red or blue shifted frequencies picked up by the telescope along a line of sight, corresponding to a variety of distances from the observer and so from the galactic core. As we are interested in getting a clear picture of the relationship between distance from the galactic core and velocity, we need to pinpoint one such pairing of distance and speed. Thankfully this is possible for galactic longitudes -90< θ_l <90 and at distances for which the angular velocity does not increase with increasing distance from the galactic core (or equivalently where the velocity does not increase faster than linearly as a function of distance). While this last condition is commonly mentioned, it is less commonly pointed out that there are regions close to the galactic core where this assumption is invalid. Thankfully for us, our observation plan starts just beyond these distances from the core.

Assuming these conditions are met, the diagram below shows the basic idea for identifying a distance and velocity pair from the wider spectrum of data. Essentially, the point with the fastest relative velocity and hence greatest blue/red shift occurs where the velocity vector is aligned with our line of sight. In other words, for the circular path that the line of sight is tangent to. This is because for points closer or farther away from us, less of the overall speed is directly toward or away from us and thus has less of a Doppler Shift. This is true even if speed increases a bit with distance from the galactic core so long as our assumptions hold above. *Therefore the greatest relative velocity observed is associated with the tangent point, which is also the closest point to the galactic core along our line of sight.* This distance can be found with simple trigonometry, and the relative velocity can be found directly from the blue or red shifting as described in the previous section.
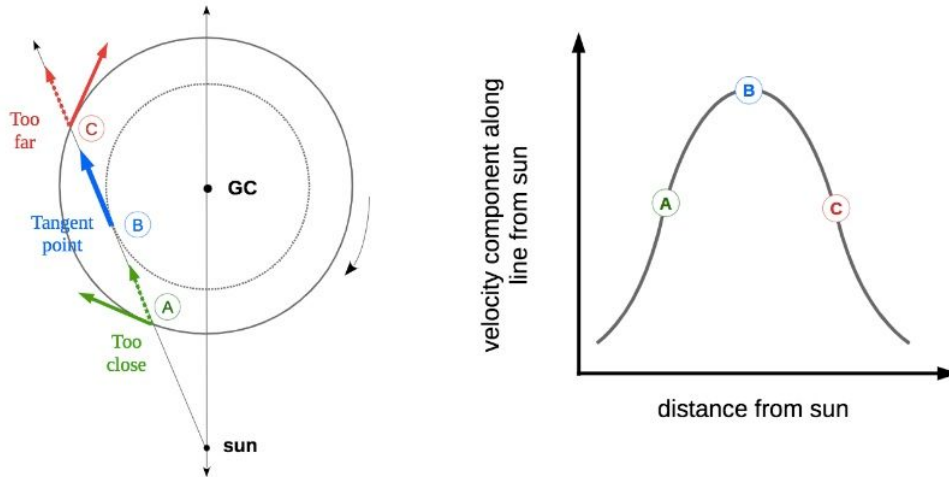
The Galactic Rotation Curve: Velocity and Distance using the Tangent Point Method

The velocity vector of the tangent point relative to the galactic core is the sum of the velocity of the tangent point relative to the sun (whose magnitude we determine from our observations) plus the velocity vector of the sun relative to the galactic core (whose magnitude is approximately 220 km/s). Mathematically this is stated more concisely as:

$$\boldsymbol{v}_{tp/gc} = \boldsymbol{v}_{tp/s} + \boldsymbol{v}_{s/gc}$$
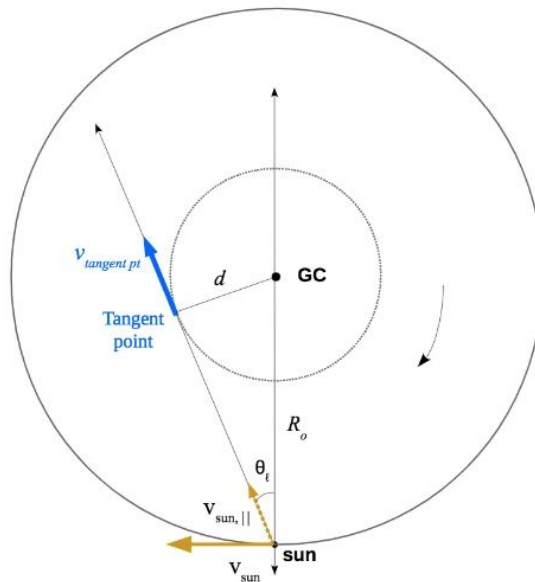
In order to determine the speed of the tangent point relative to the galactic core, we only need to focus on components of motion in that direction (i.e. parallel). Thus for the positive galactic longitude values under consideration:

$$v_{tp/gc} = v_{observed} + v_{sun,||} = v_{observed} + v_{sun}\cos(90 - \theta_l) = v_{observed} + v_{sun}\sin(\theta_l)$$

Furthermore it is clear from the geometry that

$$d = R_0 \sin(\theta_l)$$

where $R_0 = 8.0$ kpc is the distance of the Sun from the center of the galaxy.

The Galactic Rotation Curve: Observation Data

| Galactic Long. θ_l	Distance from G.C. d (kpc)	Peak Observed Rel. Vel. $v_{observed}$ (km/s)	Sun's velocity toward tangent point $v_{sun,\parallel}$ (km/s)	Velocity of tangent point rel to G.C. $v_{tp/gc}$ (km/s)
25	3.4	117.4	93	210.4
35	4.6	106.8	126	232.8
45	5.7	73.1	156	229.1
55	6.6	68.8	180	248.8
65	7.3	47.7	199	246.7
75	7.7	20.2	212	232.2

The Galactic Rotation Curve: Adjusting for Earth's Velocity Relative to the Sun

If the velocity of the Earth is not included then error bars of at least 30 m/s (the Earth's speed relative to the Sun) must be included. This is somewhat unsatisfying. In addition, we are near enough to the Autumnal Equinox that the Earth is roughly moving away from the line of sight, which would cause the measured values to be *higher* than the true value once corrected. Looking at the graph above, this matches up well with the fairly consistent vertical offset.

Trying to directly calculate the parallel contribution of Earth's velocity, I was not satisfied with the quality of information I could find and certainly had no way to quantify the error. It took a while before remembering the example of the example spectrum of Mirfak shown several pages prior: the offset of the peak of the spectrum from 1420.40575 MHz is due to in-line component of the velocity of the Earth relative to hydrogen gas in our locale, and so approximately relative to the Sun. Granted, this gas is not static relative to the Sun, but on average should match the Sun's velocity according to our simplified model of galactic motion. The shifted peaks all increased the redshift, with the amount increasing for smaller galactic longitudes, matching with the understanding that at the Autumnal Equinox the Earth velocity relative to the Sun is pointing away from the galactic core.

Galactic Long. θ_l	Distance from G.C. d (kpc)	Raw velocity of tangent point $v_{tp/gc}$ (km/s)	Estimated parallel component of Earth's velocity	**Adjusted velocity of tangent point** $v_{tp/gc}$ **(km/s)**
25	3.4	210.4	16.2	**194.2**
35	4.6	232.8	14.6	**218.2**
45	5.7	229.1	12.6	**216.5**
55	6.6	248.8	10.2	**238.6**
65	7.3	246.7	7.6	**240.1**
75	7.7	232.2	4.6	**227.7**

At last we can plot our measurements versus those of more reputable sources. Pretty darn good!
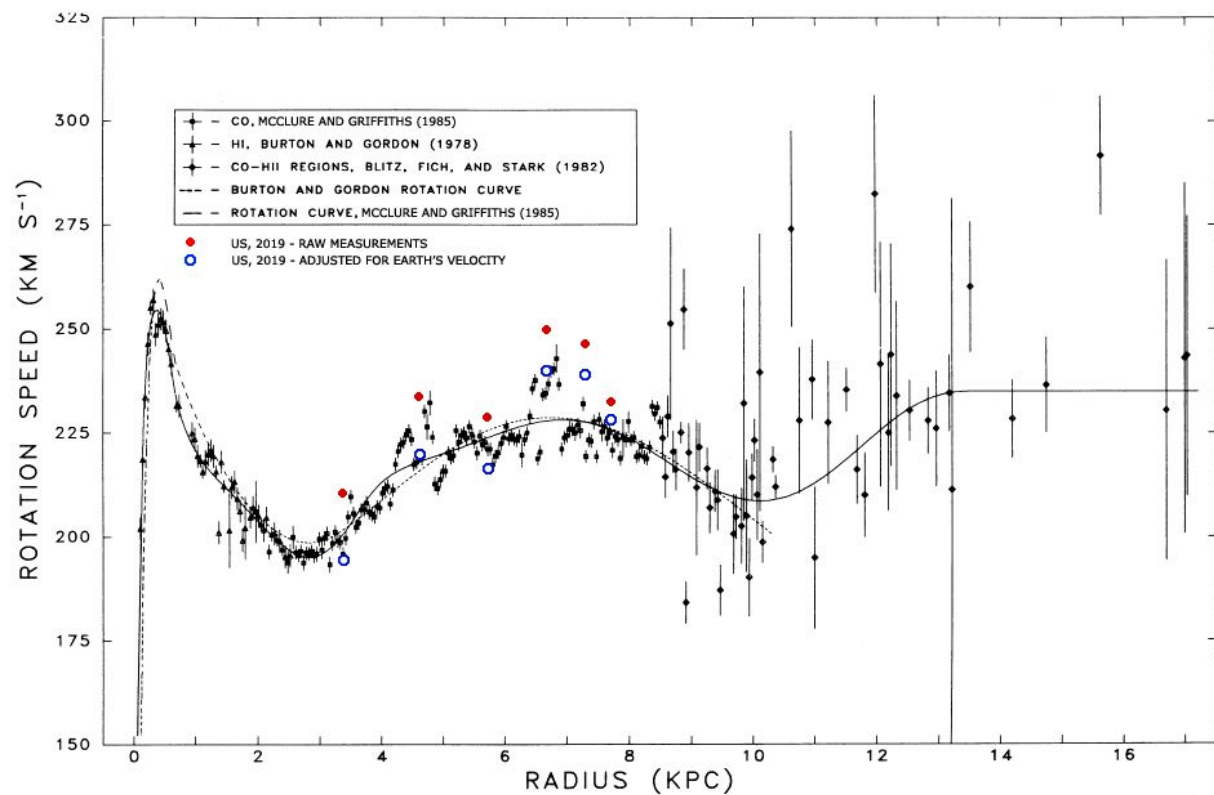
TBD:
- What are our error bar values and why?
- The connection to dark matter

Story and Song: Conclusion

Summary of Results

The accuracy of the results are quite surprising, particularly when compared to established measurements and not the best fit line. To be honest, I feel that there are some different sources of error that cancel each other out. The first of these is the fairly wide beam width of the device. This means that the highest relative velocity along a given line of sight has a good chance of being inflated due to picking up signals from smaller galactic longitudes than a straight line would suggest. Offsetting this is the noise floor from the fairly short collect times used. This would have the effect of obscuring the true maximum velocity within the noise, making the first noticeable peak have a smaller redshift than the true maximum, and thus a lower relative velocity. Since the half power beam width is ~11°, it seems like the first effect is totally unavoidable, while the second seems very probable. Given these assumptions and the accuracy of the results, it seems reasonable that these effects were both present and served to cancel each other out. Regardless, success!
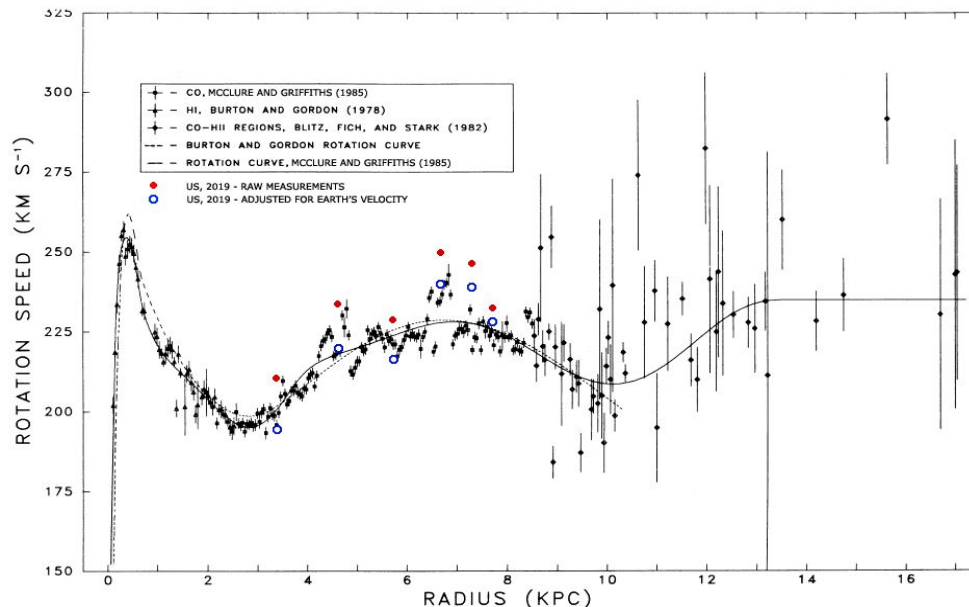
Lessons Learned

- Always use an LNA. It is amazing how the noise factor of the entire system depends on that of the first piece of equipment connected to the antenna. Even if the SDR alone can provide enough gain, just throw an LNA in front of it.
- At the boundary between academics and the DIY community, no single reference comes close to being sufficient. So, before anything else, immediately write down the section/link/page number of exactly the piece you need to a top level document along with a sentence or two describing it. I can't even fathom how much time was spent going through the same folders and books.
- Radio astronomy, radio in general, and digital signal processing are entire worlds unto themselves. In hindsight I don't think we even knew what a radio telescope really did and the situation has only marginally improved.

Classroom Applications

Aside from the obvious answer of having an astronomy class, there are potential links to other classes within and outside of the science department.

- AP Physics C - Relative velocity, uniform circular motion in the Galactic Rotation Curve calculations. Gravitation relates as well, including the suggested existence of Dark Matter.
- Physics 9 - Light, frequencies and wavelength, closed pipe standing waves, Doppler shift.
- Chemistry - Spectrometry, Hydrogen structure.
- Engineering - Quarter wave antennas, amplification, filtering, horn design and construction.
- Statistics - Averaging to extract weak signals hidden in white noise.
- PreCalc - The trigonometry needed for the galactic rotation curve, coordinate changes.

Cheesy Ending

Admittedly we're not making any new discoveries here, and it's boba in place of traditional iced tea. There are bigger and better telescopes that require many millions of dollars and hundreds of people to operate that actually advance human knowledge. But, two people with some spare time, a bit of background, a disorganized stack of references, a slightly less disorganized pile of tools and lumber, radio equipment they didn't know how to use, and a vague notion that somehow a radio telescope could be made out of all of this actually figured out how and (sort of) why this thing works. Two months ago we knew we live in a spiral arm galaxy because someone told us; now we can see it using something we built ourselves. So, even if our "I wonder *how* ..." is <u>much</u> more modest than the "I wonder *if* ..." of the scientists of yesteryear, it is still satisfying to have a question and be able to answer it ourselves, especially if it means we can look across the galaxy to do so.

Here There Be Gerblins: References

Digital Signal Processing in Radio Astronomy (DSPIRA):
- [Program Description and Objectives](#)
- [Primary Website](#)
  - [Lectures](#)
  - [Labs](#), primarily describing GnuRadio projects building up from basic radio to the spectrometer, but also including the construction plans used here.
- [GitHub Repository](#)

Open Source Radio Telescopes:
- [Hydrogen Line Telescope Plans and Procedures](#)
- [LightWork Memo Series](#), a look at the development behind the designs. Memos 14 and up are particularly relevant.

Radio Astronomy:
- Condon, James J., and Scott M. Ransom. *Essential Radio Astronomy*. Vol. 2. Princeton University Press, 2016. ([Full text](#)) Ch.3. on Antennae, Radiometers/Spectrometers and Ch.7 on Hydrogen Line are particularly helpful.

Digital Signal Processing and Software Defined Radio:
- Owen, Mark. *Practical Signal Processing*. Cambridge University Press, 2007.
- Clark, Paul, and Clark, Davis. *Field Expedient SDR*. Vols. 1-3. CreateSpace Independent Publishing Platform, 2016.
- Ossmann, Michael. *Software Defined Radio with HackRF.* Online video series: https://greatscottgadgets.com/sdr/
- [RTL-SDR.com](#) for all sorts of othee SDR project ideas

Similar Projects:
- Patel, et. al. *A low-cost 21 cm horn-antenna radio telescope for education and outreach.* https://www.cfa.harvard.edu/~npatel/hornAntennaAASposterPDF2.pdf

Antenna Design and Analysis:
- Nikolova, Natalia. *Lecture Notes: Antenna Engineering*. McMaster University. http://www.ece.mcmaster.ca/faculty/nikolova/antenna_dload/current_lectures/LectureNotesAntennas_Nikolova.pdf, Chapter 18.
- *Essential Radio Astronomy*, Chapter 3.

Velocity Curve Calculation Examples:
- http://www.astro.wisc.edu/~sstanimi/Students/rotation.pdf
- *Essential Radio Astronomy*, Chapter 7.